water

MDPI

Article

On the Relationship between Aquatic Plant Stem Characteristics and Drag Force: Is a Modeling Application Possible?

Anna Maria Łoboda [1], Mikołaj Karpiński [1] and Robert Józef Bialik [2,*]

[1] Institute of Geophysics, Polish Academy of Sciences, Księcia Janusza 64, 01-452 Warsaw, Poland; aloboda@igf.edu.pl (A.M.Ł.); mkarpin@igf.edu.pl (M.K.)
[2] Institute of Biochemistry and Biophysics, Polish Academy of Sciences, Pawińskiego 5a, 02-106 Warsaw, Poland
* Correspondence: rbialik@ibb.waw.pl; Tel.: +48-22-592-5796

Received: 22 March 2018; Accepted: 20 April 2018; Published: 24 April 2018

Abstract: This paper presents a basic model that shows the relationship between the diameter of a stem and its flexural rigidity. The model was developed from experimental measurements of biomechanical traits (i.e., tensile and bending traits like maximum forces, stresses, moduli of elasticity, flexural rigidity, strain) of three freshwater macrophyte species (*Elodea canadensis* Michx., *Potamogeton pectinatus* L., and *P. crispus* L.), reflecting the seasonal changes in plant biomechanics throughout the vegetative season. These were obtained with the use of a bench-top testing machine in 2016 and 2017. The presented calculations are based on the ratio of drag-to-bending forces, in which the flexural rigidity plays a key role. The proposed model has the form $EI = ad^b$, and two approaches based on a regression analysis were applied to determine the parameters of the model—a and b. In the first method, the parameters were identified separately for each day of measurement, while in the second method, the coefficient b was calculated for all data from all days as a unified number for individual plants. The results suggest that coefficient b may provide information about the proportion of changes in drag forces depending on plant stiffness. The values of this coefficient were associated with the shape of the stem cross-section. The more circular the cross-section, the closer the value of the parameter was to 1. The parameter values were 1.60 for *E. canadensis*, 1.98 for *P. pectinatus*, and 2.46 for *P. crispus*. Moreover, this value also depended on the density of the cross-section structure. Most of the results showed that with an increase in stem diameter, the ratio between the drag and bending forces decreased, which led to fewer differences between these two forces. The model application may be introduced in many laboratory measurements of flow–biota interactions as well as in aquatic plant management applications. The implementation of these results in control methods for hydrophytes may help in mitigating floods caused by increases to a river channel's resistance due to the occurrence of plants.

Keywords: aquatic plants; biomechanics; drag force; hydrodynamics; flow–biota interactions; hydrological processes

1. Introduction

Aquatic plants that grow in rivers significantly affect hydrological conditions, e.g., [1–5]. Estimations of hydraulic resistance [4,6,7], stream restoration [8–10], investigations of invasive aquatic plant colonization [11,12], and development of theoretical approaches for linking ecological, biomechanical, and hydrodynamic descriptions [1,2,13] play important roles in the development of the ecological management of vegetated channels, both separately and as components of aquatic

interfaces. The interaction mechanisms between plants and flow structures may be considered on multiple interconnected scales, such as leaf, stem, individual plant, plant patch, or plant patch mosaic scales [1,14]. These interactions depend on the geometry and mechanical properties of aquatic macrophytes [1]. The comprehensive knowledge of these interplays consists of three groups of plant characteristics [1]: (1) plant morphology characteristics; (2) plant material characteristics; and (3) flow–plant interaction characteristics (Figure 1). Plant morphology characteristics include information about plant geometry (e.g., length, width, cross-sectional area) as well as about plant density (e.g., number of individuals per unit bed area). Plant material characteristics provide details about the mechanical behaviors of hydrophytes, such as flexural rigidity, modulus of elasticity, or mechanical strength. The third set of characteristics quantifies the interaction between plants and water flow and includes characteristics such as the drag coefficient [1]. The connection of these features (Figure 1) may open a new avenue in studies of flow–biota interactions [1], and yet determining this connection is still a challenge for scientists focusing on freshwater ecosystems research.

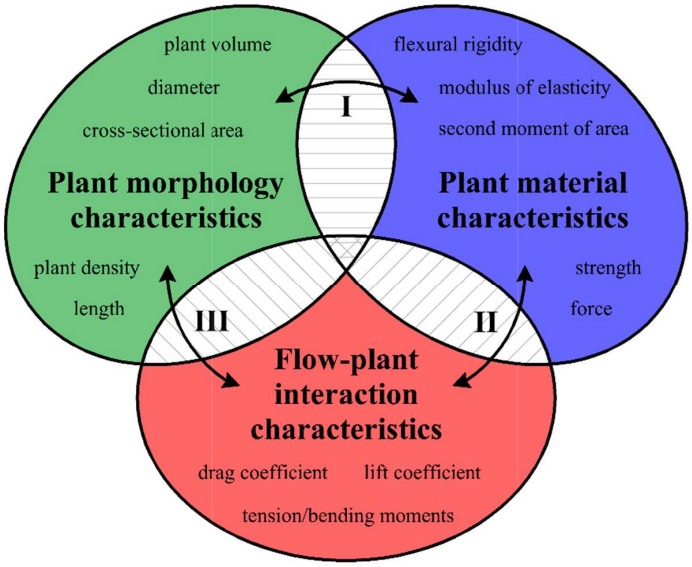

Figure 1. A schematic of the divisions of plant characteristics.

The study of the interplay between plants and flow structures is based on several forces, i.e., flow-induced, plant-induced, and plant-reaction forces, which need to be considered because they control the flow regime of a vegetated river [1]. The main loads acting upon a plant stem are the drag force, the buoyancy force, and the gravity force (Figure 2), which cause the plants to bend in the direction of water flow, which increases the tension of a shoot. To extend the scope of research focusing on the hydrodynamics of aquatic ecosystems, Nikora et al. [15], Nikora et al. [16], and Larned et al. [17] suggested the application of similarity numbers concentrating on the ratios of these forces, and some of these numbers have been used to model flow–organism interactions and mass-transfer processes. The flow–plant similarity numbers have been broadly described by Nikora [1], who highlighted the importance of a comprehensive approach in aquatic ecosystems. Although some achievements have been made with the use of plant biomechanics and similarity numbers, e.g., [18–20], progress in this area has been slowed by the limited information on the biomechanical properties of aquatic macrophytes [1]. For example, Ghisalberti and Nepf [20] used two similarity numbers, focusing on a combination of the buoyancy force, the elastic force, and the drag force, for simulations of eelgrass meadows in laboratory conditions. On the other hand, Usherwood et al. [19] developed simple expressions for drag based on the plant shoot length or flow speed, which showed that for a fixed length, the drag force changed linearly to the flow speed and for the fixed velocity it changed linearly to the shoot length.

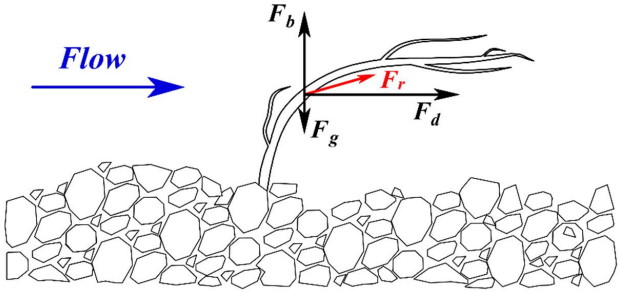

Figure 2. The main forces acting upon a plant stem: the drag force F_d, the buoyancy force F_b, the gravity force F_g, and the resultant force F_r.

Although it has been almost a decade since the problem was formulated, studies on the links between the forces acting on flow–biota interactions are still in their infancy, and the uses of these links are rare due to difficulties. Even though there have been achievements in particular groups of characteristics, a function that links all components together has not been acquired. Aquatic plant morphology provides information about the geometry and internal structure of plants, e.g., [21], yet the determinations of these characteristics are not completely connected with the characteristics of other groups (connection I or III in Figure 1). Field experiments provide a great opportunity to investigate plant densities or volumetric characteristics to develop a database of these traits. However, this approach is not fully utilized by researchers, which causes problems for the synchronization of flow–biota studies in aquatic ecology. According to the plant material characteristics of freshwater macrophytes, research on these traits is still rare and needs to be extended due to their influences on river processes [1,22,23]. A large amount of research has focused on marine plant species such as seagrasses [24–27] or seaweeds [28–31]. However, less attention has been given to freshwater macrophytes [19,22,23,32–36]. Nevertheless, some progress in this area has been made. For example, according to suggestions noted by Schutten et al. [37] and Miler et al. [34] about the changes in biomechanical properties throughout the life cycle of a plant, seasonal variations of these traits have been investigated throughout the growing season [35,36]. Seasonal changes in biomechanical properties have been proven for selected plant species, i.e., *E. canadensis* [35] and *Potamogeton* spp. [36]. Furthermore, much of the research has concentrated on drag coefficients and the hydraulic resistance generated by vegetation, e.g., [6,38–40]. Nikora et al. [6] examined the effects of aquatic plant biomass, stature, and architecture on hydraulic performance. They noticed that the roughness may be obtained from plant morphology characteristics. Moreover, Sand-Jensen [38] suggested that drag, which is caused by flexible, submerged macrophytes, may increase in direct proportion to water velocity, whereas in the vicinity of rigid vegetation, the flow resistance increases proportionally, at least, to the square root of velocity. Although there have been many attempts to model the interactions between plants and turbulent flow in a laboratory, e.g., [41–45], similar experiments in the field are not common, e.g., [6]. Thus, the transfer of laboratory knowledge to real conditions is a challenge that needs to be addressed.

Even though the flow–organism interplays are well known and understood [40], there are extensive knowledge gaps in the investigations that link the fluid mechanics, biomechanics, and ecology [1,2,13]. The proper connection of these three components of plant characteristics and the affected hydrological processes in vegetated channels is still unknown. One important relationship is the correlation between drag and bending forces [1], which depends mostly on plant morphology characteristics and a key material parameter that alters the drag force and the rate of mass flux and affects the fluid velocity [46,47], i.e., the flexural rigidity. According to Tymiński and Kałuża [3] and Aberle and Järvelä [4], the flexibility of a plant plays a key role in flow resistance calculations, as it defines the amount of bending under the force of flowing water. Hence, by understanding the plant morphology and stiffness components, we may be able to estimate the total drag due to the existence

of aquatic plants, which is one of the most important and influential parameters in the construction of dams or other water structures, as well as river management in the ecological or engineering sense in vegetated rivers [48–50]. In addition, the improvement in knowledge about plant characteristics may allow for the proposition of new control methods for hydrophytes, as they cause flooding due to the increase in the resistance of rivers [19,51,52], which is also influential from the perspective of hydraulic engineering.

The present study is focused on extending the research of flow–biota interactions at the scale of the plant stem. The main objective is to provide a basic model that shows a correlation between the diameter of a stem and its flexural rigidity using examples from three freshwater macrophyte species while focusing on changes in plant biomechanics throughout the vegetative season [35,36]. An additional goal of this paper is to determine whether or not there is any possibility to obtain a formula that may help properly calculate drag forces based on the information available about the phenological state of an aquatic plant, which could be obtained from the biomechanical properties of the plant.

2. Materials and Methods

2.1. Theoretical Assumptions

The theoretical foundation of our considerations is based on the relation between the drag force due to the existence of a plant in the river channel F_D and the bending force of this plant F_B. The description of this ratio was proposed by Nikora [1] in the following form:

$$\frac{F_D}{F_B} = \frac{0.5 \cdot \rho \cdot C_D \cdot U^2 \cdot A \cdot R \cdot \lambda}{EI}, \quad (1)$$

where ρ is the plant density, C_D is the drag coefficient, U is the reference velocity, A is the reference plant area, R is the radius of curvature at a point where the bending force is defined, λ is the distance from the bed to the point where the resultant fluid force acts, and EI is the flexural rigidity. Referring to Figure 1, most of these parameters depend on the material characteristics of the plant, which have not yet been investigated in relation to the biomechanical traits of plants. Thus, our calculations focused on the stem diameter, which is easily measured and could be used to determine the phenological development stage of a plant.

The following assumptions were used to set up the model:

1. The flexural rigidity EI, which has a constant modulus of elasticity E [MPa] for solid materials with a circular cross-sectional shape, is expressed as [53]

$$EI = E \cdot I_C = \frac{E \cdot 3.14 \cdot d^4}{64} \cong 0.05 \cdot E \cdot d^4, \quad (2)$$

   where I_C is the second moment of area for the circular cross-section and is defined as $I_C = \frac{\pi d^4}{64}$, [mm^4], and d is the stem diameter [mm].
2. When the cross-section of the stem plant has a circular shape (the ideal situation), the second moment of area I depends on the plant diameter d to the fourth power, i.e., $I \sim d^4$. This condition is true even in the case when the shape scales with the increase in diameter—that is, when the cross-sections are similar (in the sense of the similarity of the figures). On the other hand, stems of aquatic plants do not have uniform cross-sections or perfect circular shapes (Figure 3). To simplify the biomechanical measurements, the cross-sectional area of the stem is usually compared to a specific shape with a solid structure [35,36]. However, a plant stem is not a solid material. The internal structure of a plant is more complex and it is not uniform for the plant's entire lifecycle. In addition, a cross-sectional area does not change proportionally with the increase in diameter. Hence, the assumption of diameter to the fourth power as described by Equation (3)

that is used for solid materials is not correct for biological systems. Therefore, in our nonideal situation, the second moment of area is approximately $I \sim F(d)\ d^4$, where $F(d)$ is a function of the shape, which, in turn, is a function of time $d(t)$, as hydrophytes change their dimensions throughout the growing season. In addition, we assume here that the shapes of cross-sections of plants with the same diameters are (roughly) the same.

3. In the ideal situation, flexural modulus E does not depend on the plant diameter. E is the property of the material from which the plant was "built". However, our situation is not ideal, and when the plant grows, the material from which it was built changes. Thus, again, $E \sim H(d, t)$.

We can combine these three model assumptions and obtain the following formula:

$$EI \sim F(d,t) \cdot H(d,t) \cdot d(t)^4, \tag{3}$$

where EI is proportional to the functions of diameter and time.

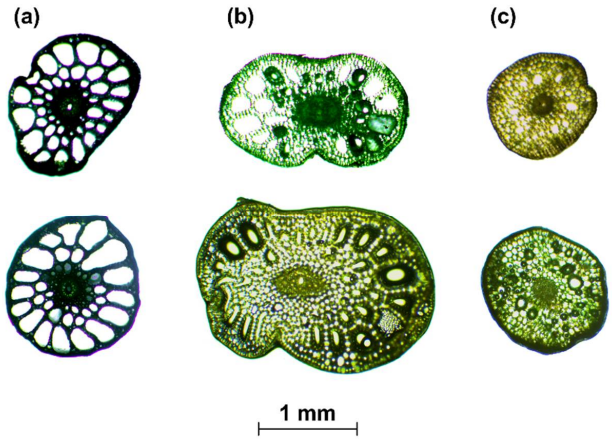

Figure 3. Examples of cross-sections of aquatic plants: *P. pectinatus* L. (**a**), *P. crispus* L. (**b**), *E. canadensis* Michx. (**c**). (**a**,**b**) were modified from Łoboda et al. [36].

Based on the aforementioned assumptions, we can suggest that the relationship between the modeled flexural rigidity EI_m and the stem diameter d has the following form:

$$EI_m = ad^b, \tag{4}$$

where a and b represent the coefficients of the model that are calculated using a nonlinear regression. The power function was chosen due to monotonicity of the plant diameter data. However, as presented in Equation (3), the plant biomechanics change throughout the life cycle [35,36]. The coefficient a is a function of flexural modulus that, in turn, is dependent on diameter and time (growing season). Thus, a is responsible for changes in the biomechanical traits and morphology of a plant during growth. Łoboda et al. [35,36] investigated whether there were differences in biomechanical parameters obtained during two periods and if these changes were statistically significant or not. The studies confirmed seasonal fluctuations in tension and bending properties, which impact correct calculations of the flow resistance. On the other hand, the coefficient b defines morphology characteristics that vary between plant species and periods of the growth stage, i.e., it defines how the cross-sectional area and diameter change the flexural rigidity at a certain time in the life cycle of a plant.

2.2. Data

The biomechanical data used in this investigation were collected with a Tinius Olsen Bench Top Testing Machine 5ST (Tinius Olsen, Redhill, UK) using the Horizon software (a detailed description of the method is in Łoboda et al. [23], and the data used in this study are described in Łoboda et

al. [35,36]). The plant collection and measurements were carried out in 2016 and 2017 over the course of the entire plant growth season from the Wilga River, Poland (51°51′30″ N, 21°28′20″ E, Figure 4), where the flow speed was approximately 0.5–0.7 m·s^{-1} [36]. The Wilga River is a lowland river, and the bed of the river is mostly covered with medium and coarse sand [36,54]. The channel bed at the sampling site, which is in a natural unregulated part of the river, is strongly vegetated by aquatic plants, containing small stones and gravel [36].

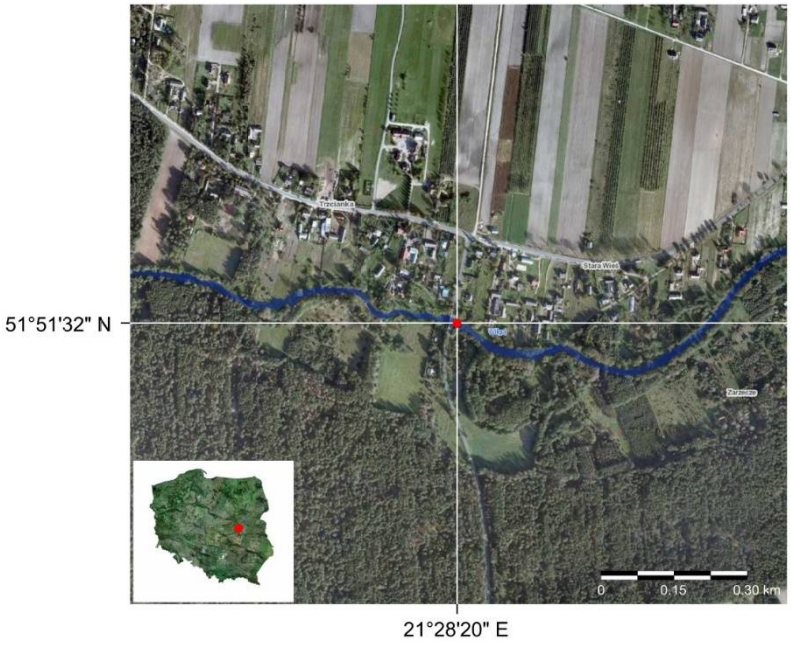

Figure 4. Sampling site on the Wilga River indicated by the red point.

2.3. Regression Calculations

We simplified Equation (3) and determined the parameters a and b in Equation (4) based on the data from biomechanical laboratory measurements for three freshwater macrophyte species: *E. canadensis*, *P. pectinatus*, and *P. crispus*, [35,36]. Two cases were investigated.

In case 1, the coefficients a and b were separately calculated using data from different days. Simply, the function from Equation (4) was minimized by the a and b values in the following function:

$$\min_{a,b} |EI_m - f(d)|^2. \quad (5)$$

In contrast to case 1, the coefficient b was calculated in case 2 for all data from all days as a unified number for the individual plant, and the coefficient a, in this case, was calculated based on the mean squared error (MSE) value. In other words, Equation (4) was minimized by $a_1, \ldots, a_n$ and b values in the following function based on the whole dataset:

$$\min_{a_{1,,}\, a_n, b} |EI_m - f(d)|^2. \quad (6)$$

3. Results

3.1. Regression Analysis

3.1.1. Case 1

The coefficient a for *E. canadensis* varied from 2.22 to 10.32 depending on the measurement date (Table 1). The highest value was observed on 16 August 2016, which coincided with the highest

biomechanical properties of the plant (e.g., flexural modulus E, Table 1) at this time [35]. On the other hand, the coefficient *b* for this species was characterized by lower dispersion from 1.14 to 2.31 (Table 1). The parameter *b*, which is responsible for the plant geometry, had a smaller influence on the final result of flexural rigidity for samples with higher flexural modulus values. Moreover, the differences in flexural rigidity between periods for samples were also more dependent on the variation in the modulus of elasticity (Table 1). For *P. pectinatus*, the calculations of parameter *a* showed values from 1.74 on 13 September 2016, when the plant had low flexural rigidity, to 16.32 on 14 June 2017. The high values of coefficient *a* were in line with the very small values of coefficient *b*, which varied from 0.07 to 4.32 (Table 1). The third investigated aquatic macrophyte species, *P. crispus*, was characterized by the largest scatter of calculated parameters (Table 1). The maximum coefficient *a* was equal to 20.86 and was estimated for the data from 16 August 2016 when the plant reached the highest flexural modulus, whereas the lowest value was 0.01 (Table 1). The parameter *b* varied from 0.27 to 9.90 (Table 1).

Table 1. Outcomes of the coefficients *a* and *b*, the mean stem diameter *d* and the mean flexural modulus E for *E. canadensis*, *P. pectinatus* and *P. crispus* for two cases throughout the growing season. MSE is the mean squared error. * data from Łoboda et al. [35]; ** data from Łoboda et al. [36].

E. canadensis									
Date of Collection	**Mean Stem Diameter ***	**Mean Flexural Modulus ***	**Case 1**			**Case 2**			**MSE Relative Diff.**
	[mm]	**[MPa]**	***a***	***b***	***MSE***	***a***	***b***	***MSE***	**[%]**
2016-06-09	1.07	62.54	3.47	2.20	6.51	3.67		6.58	1.08
2016-06-24	1.10	95.32	3.36	1.93	8.19	5.59		8.23	0.49
2016-08-16	1.18	141.20	10.32	1.14	7.64	9.47	1.60	7.97	4.32
2016-09-13	1.37	60.07	5.49	2.03	75.86	6.36		76.09	0.30
2016-10-04	1.24	32.31	2.22	2.31	2.27	2.63		2.33	2.64
P. pectinatus									
Date of Collection	**Mean stem Diameter ****	**Mean Flexural Modulus ****	**Case 1**			**Case 2**			**MSE Relative Diff.**
	[mm]	**[MPa]**	***a***	***b***	***MSE***	***a***	***b***	***MSE***	**[%]**
2016-05-14	1.30	94.51	7.93	1.10	49.70	5.41		55.99	12.66
2016-06-09	0.97	86.59	2.93	2.66	6.39	3.45		6.75	5.63
2016-06-24	1.37	90.18	11.16	0.24	62.14	5.26		81.85	31.72
2016-08-16	1.56	94.09	7.26	2.17	212.51	8.20		213.32	0.38
2016-09-13	1.68	36.66	1.74	3.31	49.88	4.44		54.80	9.86
2016-10-04	1.26	55.08	4.26	0.98	30.49	2.91	1.98	32.43	6.36
2017-06-14	1.22	168.50	16.32	0.07	26.49	10.35		43.03	62.44
2017-07-12	0.84	252.97	6.55	4.32	14.71	9.70		31.96	117.27
2017-08-08	1.21	109.72	8.89	0.28	8.04	5.75		13.19	64.05
2017-10-31	1.24	117.56	6.77	2.02	18.15	6.90		18.17	0.11
2017-11-21	1.17	174.56	9.18	2.69	43.26	11.49		50.22	16.09
P. crispus									
Date of Collection	**Mean Stem Diameter ****	**Mean Flexural Modulus ****	**Case 1**			**Case 2**			**MSE Relative Diff.**
	[mm]	**[MPa]**	***a***	***b***	***MSE***	***a***	***b***	***MSE***	**[%]**
2016-05-14	2.10	33.54	13.28	0.89	261.59	3.57		299.24	14.37
2016-06-09	2.43	19.78	0.12	6.29	395.53	4.16		451.57	14.18
2016-06-24	1.87	51.59	14.99	0.84	194.40	4.53		247.34	27.28
2016-08-16	1.97	105.21	20.86	1.65	706.28	10.82		781.83	10.69
2016-09-13	2.23	36.38	6.23	2.45	1329.52	6.17	2.46	1329.53	0
2016-10-04	2.21	43.17	0.01	9.90	349.31	7.06		1062.55	204.18
2016-11-04	1.84	55.22	2.17	4.10	275.05	7.09		323.51	17.64
2016-12-06	1.70	52.71	8.64	1.35	239.71	4.57		248.21	3.55
2017-08-08	1.90	38.50	12.93	0.29	51.47	2.56		81.82	59.14
2017-11-10	1.65	77.41	20.40	0.27	54.41	5.72		114.66	110.85

3.1.2. Case 2

The coefficient b for *E. canadensis* was 1.60, whereas the coefficient a varied from 2.63 to 9.47, and the directions of the variations between the tested periods were in line with the changes in the flexural modulus (Table 1). The calculations showed that the parameter b for *P. pectinatus* was 1.98. However, for the second plant from Potamogeton spp., *P. crispus*, the cross-sectional area has been likened to a different shape than for the other plants (ellipse), and the coefficient b was the highest, equaling 2.46 (Table 1). The parameter a for *P. pectinatus* varied from 2.91 to 11.49 depending on the plant growth stage, whereas the values for *P. crispus* ranged from 2.56 to 10.82 (Table 1). Moreover, the MSEs for both cases were the lowest for *E. canadensis*, and they were similar due to the lower values of the flexural rigidity EI and the smaller data span.

3.1.3. Cases Comparison

The MSE relative difference between case 1 and case 2 shows a decrease in the fitting of the function to the data from individual dates of sample collection in case 2, when the coefficient b was calculated as one value for the entire growing season of the plant. The smallest values of the MSE relative difference were obtained for *E. canadensis*, where the maximum decrease in the function fitting was 4.32% (Table 1), while the differences in regression fitting between both cases for *Potamogeton* spp. varied from 0.11% to 117.27% and from 0% to 204.18% for *P. pectinatus* and *P. crispus*, respectively (Table 1).

3.2. Data Analysis

According to Nikora [1], some of the variables in Equation (1) are a function of L (the large plant scale, e.g., length) or d (the small plant scale, e.g., diameter). Thus, $EI \propto d$, $A \propto dL$, $R \propto L$, $\lambda \propto L$, and the F_D/F_B relationship may be presented in the following form:

$$\frac{F_D}{F_B} = 0.5 \cdot \rho \cdot C_D \cdot U^2 \cdot L^3 \cdot \frac{d}{EI} \tag{7}$$

where ρ, C_D, and U are independent of the plant diameter d. In our case, $EI = a \cdot d^b$, which finally gives

$$\frac{F_D}{F_B} = \frac{0.5 \cdot \rho \cdot C_D \cdot U^2 \cdot L^3}{a} \cdot \frac{d}{d^b} = X \cdot d^{1-b} \tag{8}$$

If we assume that X is independent of the plant diameter and does not change suddenly and significantly, the coefficient b may provide information about the influence of changes in the diameter and the flexural rigidity on the ratio between the drag force F_D and the bending force F_B. For the cases when the coefficient $b \geq 1$, this ratio decreases and has positive limits equal to 0. On the other hand, in the case when the coefficient $b \in \langle 0, 1)$, the ratio increases, and it is proportional to the root function of the plant diameter. For $b = 1$, a state of equilibrium between these two forces is expected. Specifically, for case 2 (Table 1), the values of coefficient b were equal to 1.60, 1.98, and 2.46 for each sample. Substituting a specific value for this coefficient, we are able to estimate the proportion of changes in drag forces depending on the plant stiffness. More detailed descriptions of the obtained results are presented in the discussion section.

4. Discussion

One of the interdisciplinary problems of aquatic interfaces is the lack of biomechanical models for freshwater macrophytes [13]. Thus, a function (Equation (4)) along with two formulas (Equations (5) and (6)) were presented, which may help properly calculate the drag forces (Equation (1)). These calculations were used to estimate the relationship between the diameter of a stem and its flexural rigidity using examples from three freshwater macrophyte species: *E. canadensis*, *P. pectinatus*, and *P. crispus*.

In our calculations, case 1 focused on describing the investigated relationships in detail, while case 2 presented a general method where one of the coefficients was unified for the plant. Based on Equation (2), we assumed that the proposed model is powerful. Nevertheless, in the case of living material, it is questionable if this relationship is indeed powerful, but the results showed that the approximation (Equation (4)), which was also used in the measurements of Fukushima and Sato [55], seems to be correct. Moreover, the analysis was based on seasonal changes in the growth stage of hydrophytes. Thus, the functions of both the shape and modulus of elasticity, which were F and H, respectively (Equation (3)), depended on the diameter of the plant and time. Because the cross-sections of the plants have not been analyzed in detail, the model investigated the impacts of both factors, i.e., the flexural modulus and the shape of the cross-section, together. Nevertheless, our results provide an opportunity to extend the knowledge of flow–biota interfaces [13] in a general (case 2) or more specific (case 1) way. The simplification of coefficient b in case 2 generalizes the information about the morphology characteristics of individual species while maintaining the seasonal variations in material behavior [35,36]. In the *E. canadensis* example, both presented cases gave similar functions for each period (Figure 5). Thus, the model application may be carried out on a simplified method with coefficient b equal to 1.60 (Table 1). On the other hand, the differences between the results were higher from the two cases for *Potamogeton* spp. than from the *E. canadensis* example, e.g., on 4 October 2016 for *P. crispus* or 14 June 2017 for *P. pectinatus* (Figure 5). Thus, the selection of the preferred method for the processing of laboratory measurements may depend on the data and/or the expected use of the obtained results. However, most of the plant growth periods modeled in case 1 and case 2 were in a good agreement.

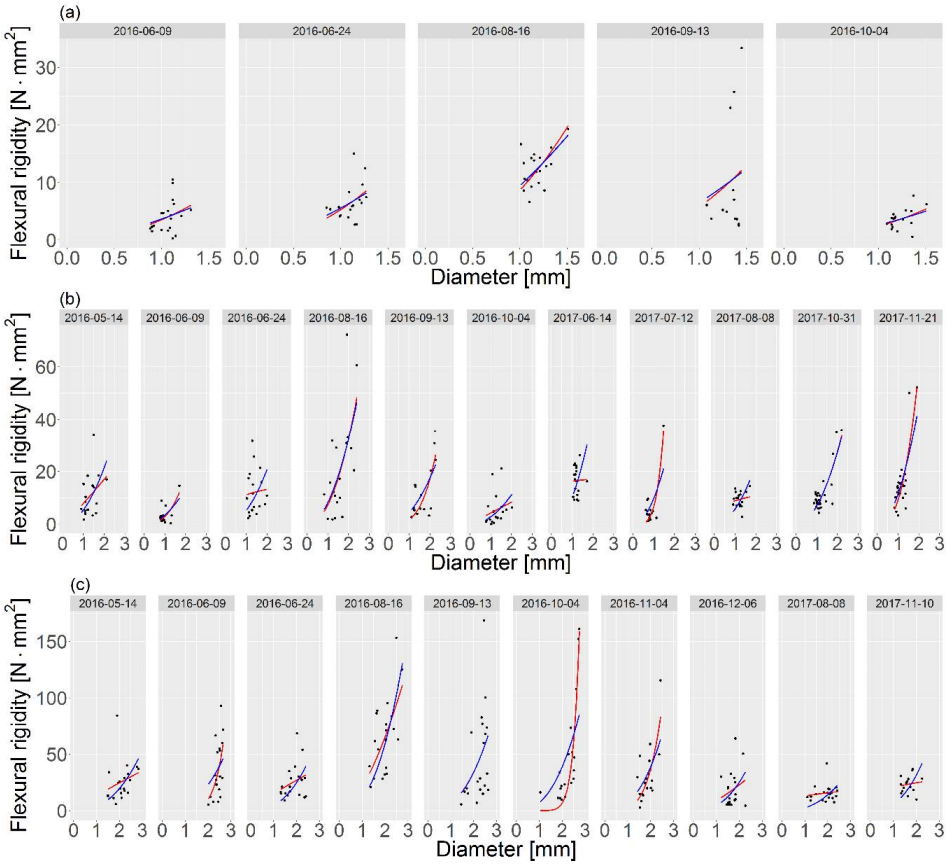

Figure 5. Model matching for *E. canadensis* (**a**), *P. pectinatus* (**b**) and *P. crispus* (**c**). The red line —— represents case 1, and the blue line —— represents case 2.

The simplified method (case 2) showed three different results for coefficient b for each plant species (Table 1). In contrast to homogeneous material with circular cross-sectional shapes where this parameter is equal to 4, the calculations revealed values of 1.60, 1.98, and 2.46 (Table 1). The differences between species may result from a variety of internal structures (Figure 3). The cross-sections of two stems (*E. canadensis* and *P. pectinatus*) resembled circular shapes; however, the coefficient b for *E. canadensis* was 1.60, and the structure of this species was denser than that of *P. pectinatus* (Figure 3). Thus, *E. canadensis* had a lower volume of air channels, which may result in lower turgor pressure, which, in turn, affects the stem stiffness [56]. The impact of the shape on the final outcomes in this species, therefore, was smaller than in *P. pectinatus* due to higher elasticity [35,36]. The internal structure of *P. crispus* reveals two overlapping circles that were likened to ellipses (Figure 3), and this plant was characterized by a higher coefficient b. However, as mentioned above, because the cross-sections of the plants were not analyzed in detail, we cannot unambiguously assume the dependence of the shape on the final result of the parameter b. On the other hand, our results may indicate that the higher the plant stiffness, the lower the influence of the flexural modulus, which is in line with the flexural rigidities of the investigated species that were calculated by Łoboda et al. [35,36]. In addition, Fukushima and Sato [55] also examined the relationship between the flexural rigidity and the diameter of living material in cabbage. In contrast to our results, where the coefficient b was lower than 4 (the value for a solid circular material), they acquired a higher value equal to 6.15, which indicated that stiffness had a greater influence on the shape of the sample cross-section than the flexural modulus. The reason for this difference could be that cabbage may have lower elasticity than hydrophytes, and thus, the modulus of elasticity should also be lower. Moreover, cabbage is an example of terrestrial plants, which are characterized by higher stiffnesses than aquatic plants [19,57]. The coefficient b also sheds light on how the proportion of changes in drag forces depends on plant stiffness. Along with the increase in the plant stem diameter, the ratio between F_D and F_B for the same value of the coefficient b (assuming that $b > 1$) decreases; thus, the difference between the drag and bending forces is proportionally lower. On the other hand, when the coefficient $b < 1$, the situation is reversed (see Equation (8)). In the case 2 example (Table 1), the results for each investigated plant species showed that the increase in diameter caused a proportionally lower influence in drag. *E. canadensis* was characterized by the highest effect of the diameter on the proportion of forces, whereas for *P. crispus*, the dimensions led to a downtrend in the ratio of forces. Interesting results were obtained for *P. crispus* in case 1, where the coefficient b was calculated for each period. Biomechanical measurements of this hydrophyte were carried out in 2016 and 2017 [36]. During the first season (2016), most of the modeled coefficients b varied between 1 and 10 with two exceptions, which were less than but close to 1 (Table 1). Thus, the majority of the periods were characterized by a downtrend in the ratio of forces with the plant expansion, whereas the second season (2017) showed that the coefficient b was approximately 0.3 (Table 1), which meant that the ratio between F_D and F_B increased proportionally to the increase in the plant diameter. Moreover, we cannot assume that the influences that the parameters have on the ratio are hidden in the assumed variable X (Equation (8)). However, a lower value of the ratio may suggest that the plant belongs to the "bending" plants category, and the plants in this category are stiffer and cause higher resistance [1].

The flexural rigidity of a plant, which is one of the most important biomechanical traits that alters the drag force and the rate of mass flux and affects the fluid velocity [46,47] was emphasized in this study. Thus, the model application may improve the estimations of hydraulic resistance due to the occurrence of plants [4,6,7]. Nikora [1] claimed that vegetation with high flexural rigidity is mainly subject to a pressure drag, while plants characterized by low flexural rigidity are exposed to viscous skin friction following the flow. According to Albayrak et al. [46], who investigated flow–plant interactions at a leaf scale, the hydrodynamic effect of flexural rigidity is more variant than the effects of leaf shape, serration, and roughness; however, flexural rigidity may modify the adaptation mechanisms of plants and flow patterns. Moreover, with the increase in leaf stiffness, a double increase in drag [46] was observed. In addition, Albayrak et al. [44] investigated the interaction between biomechanics, drag, and turbulence of stem, leaf, and shoots of a common aquatic plant, i.e., *Glyceria fluitans* (L.) R. Br.

They showed that for the same Reynolds numbers, the stem drag coefficient was two times higher than obtained for the leaves, although the average Vogel number for stems and leaves was the same, i.e., $\alpha = -0.50$. On the other hand, Zhu et al. [21] carried out a comprehensive review of the differences in leaf morphology of five submerged macrophytes species: *Potamogeton maackianus* A. Benn., *P. pectinatus* L., *P. lucens* L., *Ceratophyllum demersum* L., and *Myriophyllum spicatum* L., showing, for example, that *P. maackianus* is characterized by alternate, oblong, or linear leaves [58,59], while *P. lucens* has narrowly lanceolate leaves with a cuneate base [60]. This leads to the interesting question, which, however, is beyond the scope of this study: what is the relationship between the flow velocity and the morphology or the biomechanical properties of the leaves of different aquatic plants?

The drag force is an essential factor in adaptation strategies or reconfigurations in response to flowing water by plants [14], which are influenced by flexural rigidity [46]. The adaptations of hydrophytes in relation to higher stiffnesses allow them to survive in slow to moderately flowing waters, while flexible plants may survive in fast-flowing rivers [22]. Thus, mechanical characteristics may also be an important component of invasive plant management [12] that can improve existing methods or even invent new ones. For example, the information about plant stiffness may be used to generate appropriate levels of water movements, frequency, and power that are necessary to destroy plants. As mentioned by Hussner et al. [12], until now there has not been a single method that could be suitable for every situation. In addition, the reduction of river vegetation is a large-scale problem regarding both invasive and indigenous plants. The obtained results may be implemented in control methods for hydrophytes, which, due to increasing in the river channels resistance, cause flooding [19,51,52]. A wider knowledge of aquatic macrophytes may give the opportunity for prediction of the habitat expansion of specific species. On the other hand, the estimation of the biomechanical traits of hydrophytes may be an important component of stream restoration, as it may help in choosing the right vegetation for reduction of stream bank erosion. Thus, more extensive knowledge of the biomechanics of introduced invasive alien aquatic plants as well as indigenous species and their estimations is required.

The model may also be applied to laboratory measurements of hydrodynamic processes in vegetated channels, which were previously conducted with the use of real [7,61–64] or artificial plants [42,65–71]. However, the mechanical characteristics of the materials that were used for hydrophyte analogs and imitations are much different from the mechanical characteristics of natural plants, e.g., flexible PVC elements used to imitate *E. canadensis* have a modulus of elasticity [70] that is several dozen times higher than that of *E. canadensis* [35]. Such differences in the flexural modulus have meaningful impacts on plant stiffness (see Equation (2)), causing errors in laboratory results [64]. The presented model may improve lab experiments by providing appropriate recalculations of the obtained outcomes. In addition, it would be worth considering calculations of existing simulations, e.g., [42,71], in accordance with seasonal changes in plant properties, as artificial elements do not grow and do not alter their characteristics, imitating only one static stage.

5. Conclusions

The testing of the biomechanical properties of aquatic plants can provide valuable information about adaptations of plants to flow conditions and different environments as well as their influence on hydrodynamic processes in vegetated channels [1,13,22,33,46]. Two possibilities for obtaining the flexural rigidity of aquatic plants have been shown. The mechanical trait influenced the drag forces based on the stem diameter, which confirms our hypothesis about the possibility of acquiring a formula that links plant characteristics and the drag force. As a conclusion, the following points are presented:

(1) The relationship between flexural rigidity of aquatic plant stem and drag has the following form: $EI = ad^b$.

(2) Our work showed that two approaches may be used for estimating plant stiffness based on plant morphology in a detailed (case 1) or general way (case 2), which is needed to obtain drag forces (Equation (1)).

(3) With a constant coefficient b, the increase in the diameter of the plant stem may cause monotonous changes in the ratio of the drag and bending forces.

(4) The model may be applied in many laboratory measurements of flow–biota interactions as well as in widely understood aquatic plant management.

Author Contributions: A.M.Ł., M.K. and R.J.B. designed the study; A.M.Ł. conducted the majority of the data analysis and wrote the majority of the paper; M.K. provided the data from the models. All authors contributed to the final version of the manuscript.

Funding: This research was funded by the National Science Centre grant number UMO-2014/13/D/ST10/01123 "Field experimental investigation of hydrodynamics of water flow-vegetation-sediment interactions at the scale of individual aquatic plants".

Acknowledgments: This work was supported by the National Science Centre, Poland, Grant No. UMO-2014/13/D/ST10/01123 "Field experimental investigation of hydrodynamics of water flow-vegetation-sediment interactions at the scale of individual aquatic plants". The publication has been partially financed from the funds of the Leading National Research Centre (KNOW) received by the Centre for Polar Studies for the period 2014–2018.

Conflicts of Interest: The authors declare no conflict of interest

References

1. Nikora, V. Hydrodynamics of aquatic ecosystems: An interface between ecology, biomechanics and environmental fluid mechanics. *River Res. Appl.* **2010**, *26*, 367–384. [CrossRef]
2. Nepf, H.M. Hydrodynamics of vegetated channels. *J. Hydraul. Res.* **2012**, *50*, 262–279. [CrossRef]
3. Tymiński, T.; Kałuża, T. Investigation of Mechanical Properties and Flow Resistance of Flexible Riverbank Vegetation. *Pol. J. Environ. Stud.* **2012**, *21*, 201–207.
4. Aberle, J.; Järvelä, J. Flow resistance of emergent rigid and flexible floodplain vegetation. *J. Hydraul. Res.* **2013**, *51*, 33–45. [CrossRef]
5. Aberle, J.; Järvelä, J. Hydrodynamics of vegetated channels. In *Rivers—Physical, Fluvial and Environmental Processes*; Rowiński, P., Radecki-Pawlik, A., Eds.; GeoPlanet: Earth and Planetary Sciences; Springer: Berlin, Germany, 2015.
6. Nikora, V.; Larned, S.; Nikora, N.; Debnath, K.; Cooper, G.; Reid, M. Hydraulic resistance due to aquatic vegetation in small streams: Field study. *J. Hydraul. Eng.* **2008**, *134*, 1326–1332. [CrossRef]
7. Stephan, U.; Gutknecht, D. Hydraulic resistance of submerged flexible vegetation. *J. Hydrol.* **2002**, *269*, 27–43. [CrossRef]
8. Rood, S.B.; Samuelson, G.M.; Braatne, J.H.; Gourley, C.R.; Hughes, F.M.; Mahoney, J.M. Managing river flows to restore floodplain forests. *Front. Ecol. Environ.* **2005**, *3*, 193–201. [CrossRef]
9. Stromberg, J.C.; Beauchamp, V.B.; Dixon, M.D.; Lite, S.J.; Paradzick, C. Importance of low-flow and high-flow characteristics to restoration of riparian vegetation along rivers in arid south-western United States. *Freshw. Biol.* **2007**, *52*, 651–679. [CrossRef]
10. Jelinek, S.; Te, T.; Gehrig, S.L.; Stewarth, H.; Nicol, J.M. Facilitating the restoration of aquatic plant communities in a Ramsar wetland. *Restor. Ecol.* **2016**, *24*, 528–537. [CrossRef]
11. Moody, M.L.; Les, D.H.; Ditomaso, J.M. The role of plant systematic in invasive aquatic plant management. *J. Aquat. Plant Manag.* **2008**, *46*, 7–15.
12. Hussner, A.; Stiers, I.; Verhofstad, M.J.J.M.; Bakker, E.S.; Grutters, B.M.C.; Haury, J.; Van Valkenburg, J.L.C.H.; Brundu, G.; Newman, J.; Clayton, J.S.; et al. Management and control methods of invasive alien freshwater aquatic plants: A review. *Aquat. Bot.* **2017**, *136*, 112–137. [CrossRef]
13. Marion, A.; Nikora, V.; Puijalon, S.; Bouma, T.; Koll, K.; Ballio, F.; Tait, S.; Zaramella, M.; Sukhodolov, A.; O'Hare, M.; et al. Aquatic interfaces: A hydrodynamic and ecological perspective. *J. Hydraul. Res.* **2014**, *52*, 744–758. [CrossRef]
14. Siniscalchi, F.; Nikora, V.I. Flow-plant interactions in open-channel flows: A comparative analysis of five freshwater plant species. *Water Resour. Res.* **2012**, *48*. [CrossRef]
15. Nikora, V.I.; Goring, D.G.; Biggs, B.J.F. A simple model of stream periphyton-flow interactions. *Oikos* **1998**, *81*, 607–611. [CrossRef]
16. Nikora, V.I.; Larned, S.; Biggs, B.J.F. Hydrodynamic effects in aquatic ecosystems with a focus on periphyton. *Recent Res. Dev. Fluid Dyn.* **2003**, *4*, 41–70.

17. Larned, S.T.; Nikora, V.I.; Biggs, B.J. Mass-transfer-limited nitrogen and phosphorus uptake by stream periphyton: A conceptual model and experimental evidence. *Limnol. Oceanogr.* **2004**, *49*, 1992–2000. [CrossRef]
18. Kouwen, N.; Unny, T.E. Flexible roughness in open channels. *J. Hydraul. Div.* **1973**, *99*, 713–728.
19. Usherwood, J.R.; Ennos, A.R.; Ball, D.J. Mechanical and anatomical adaptations in terrestrial and aquatic buttercups to their respective environments. *J. Exp. Bot.* **1997**, *48*, 1469–1475. [CrossRef]
20. Ghisalberti, M.; Nepf, H.M. Mixing layers and coherent structures in vegetated aquatic flows. *J. Geophys. Res.-Ocean.* **2002**, *107*. [CrossRef]
21. Zhu, G.; Yuan, C.; Di, G.; Zhang, M.; Ni, L.; Cao, T.; Fang, R.; Wu, G. Morphological and biomechanical response to eutrophication and hydrodynamic stresses. *Sci. Total Environ.* **2018**, *622*, 421–435. [CrossRef] [PubMed]
22. Miler, O.; Albayrak, I.; Nikora, V.; O'Hare, M. Biomechanical properties of aquatic plants and their effects on plant-flow interactions in streams and rivers. *Aquat. Sci.* **2012**, *74*, 31–44. [CrossRef]
23. Łoboda, A.M.; Przyborowski, Ł.; Karpiński, M.; Bialik, R.J.; Nikora, V.I. Biomechanical properties of aquatic plants: The effect of test conditions. *Limnol. Oceanogr. Meth.* **2018**. [CrossRef]
24. Patterson, M.R.; Harwell, M.C.; Orth, L.M.; Orth, R.J. Biomechanical properties of the reproductive shoots of eelgrass. *Aquat. Bot.* **2001**, *69*, 27–40. [CrossRef]
25. Koch, E.W.; Ackerman, J.; van Keulen, M.; Verduin, J. Fluid dynamics in seagrass ecology: From molecules to ecosystems. In *Seagrasses: Biology, Ecology and Conservation*; Larkum, A.W.D., Orth, R.J., Duarte, C.M., Eds.; Springer: Berlin, Germany, 2006.
26. Davies, P.; Morvan, C.; Sire, O.; Baley, C. Structure and properties of fibres from sea-grass (*Zostera marina*). *J. Mater. Sci.* **2007**, *42*, 4850–4857. [CrossRef]
27. Fonseca, M.S.; Koehl, M.A.R.; Kopp, B.S. Biomechanical factors contributing to self-organization in seagrass landscapes. *J. Exp. Mar. Biol. Ecol.* **2007**, *340*, 227–246. [CrossRef]
28. Gaylord, B.; Denny, M.W. Flow and flexibility: I. Effects of size, shape and stiffness in determining wave forces on the stipitate kelps *Eisenia arborea* and *Pterygophora californica*. *J. Exp. Biol.* **1997**, *200*, 3141–3164. [PubMed]
29. Denny, M.W.; Gaylord, B. The mechanics of wave-swept algae. *J. Exp. Biol.* **2002**, *205*, 1355–1362. [PubMed]
30. Harder, D.L.; Hurd, C.L.; Speck, T. Comparison of mechanical properties of four large, wave-exposed seaweeds. *Am. J. Bot.* **2006**, *93*, 1426–1432. [CrossRef] [PubMed]
31. Mach, K.J.; Hale, B.B.; Denny, M.W.; Nelson, D.V. Death by small forces: A fracture and fatigue analysis of wave-swept macroalgae. *J. Exp. Biol.* **2007**, *210*, 2231–2243. [CrossRef] [PubMed]
32. Brewer, C.A.; Parker, M. Adaptations of macrophytes to life in moving water: Upslope limits and mechanical properties of stems. *Hydrobiologia* **1990**, *194*, 133–142. [CrossRef]
33. Bociąg, K.; Gałka, A.; Łazarewicz, T.; Szmeja, J. Mechanical strenght of stems in aquatic macrophytes. *Acta Soc. Bot. Pol.* **2009**, *78*, 181–187. [CrossRef]
34. Miler, O.; Albayrak, I.; Nikora, V.; O'Hare, M. Biomechanical properties and morphological characteristics of lake and river plants: Implications for adaptations to flow conditions. *Aquat. Sci.* **2014**, *76*, 465–481. [CrossRef]
35. Łoboda, A.M.; Bialik, R.J.; Karpiński, M.; Przyborowski, Ł. Seasonal changes in the biomechanical properties of *Elodea canadensis* Michx. *Aquat. Bot.* **2018**, *147*, 43–51. [CrossRef]
36. Łoboda, A.M.; Bialik, R.J.; Karpiński, M.; Przyborowski, Ł. Two simultaneously occurring *Potamogeton* species: Similarities and differences in seasonal changes of biomechanical properties. *Pol. J. Environ. Stud.* **2019**. accepted. [CrossRef]
37. Schutten, J.; Dainty, J.; Davy, A.J. Root anchorage and its significance for submerged plants in shallow lakes. *J. Ecol.* **2005**, *93*, 556–571. [CrossRef]
38. Sand-Jensen, K. Drag and reconfiguration of freshwater macrophytes. *Freshw. Biol.* **2003**, *48*, 271–283. [CrossRef]
39. Nepf, H.; Ghisalberti, M. Flow and transport in channels with submerged vegetation. *Acta Geophys.* **2008**, *56*, 753–777. [CrossRef]
40. Luhar, M.; Nepf, H.M. From the blade scale to the reach scale: A characterization of aquatic vegetative drag. *Adv. Water Resour.* **2013**, *51*, 305–316. [CrossRef]
41. Kubrak, E.; Kubrak, J.; Rowiński, P.M. Vertical velocity distributions through and above submerged, flexible vegetation. *Hydrol. Sci. J.* **2008**, *53*, 905–920. [CrossRef]

42. Kubrak, E.; Kubrak, J.; Rowiński, P.M. Influence of a method of evaluation of the curvature of flexible vegetation elements on vertical distributions of flow velocities. *Acta Geophys.* **2012**, *60*, 1098–1119. [CrossRef]
43. Hui, E.Q.; Hu, X.E.; Jiang, C.B.; Zhu, Z.D. A study of drag coefficient related with vegetation based on the flume experiment. *J. Hydrodyn.* **2010**, *22*, 329–337. [CrossRef]
44. Albayrak, I.; Nikora, V.; Miler, O.; O'Hare, M.T. Flow–plant interactions at leaf, stem and shoot scales: Drag, turbulence, and biomechanics. *Aquat. Sci.* **2014**, *76*, 269–294. [CrossRef]
45. Liu, X.; Zeng, Y. Drag coefficient for rigid vegetation in subcritical open-channel flow. *Environ. Fluid Mech.* **2017**, *17*, 1035–1050. [CrossRef]
46. Albayrak, I.; Nikora, V.; Miler, O.; O'Hare, M. Flow-plant interactions at a leaf scale: Effects of leaf shape, serration, roughness and flexural rigidity. *Aquat. Sci.* **2012**, *74*, 267–286. [CrossRef]
47. Rominger, J.T.; Nepf, H.M. Effects of blade flexural rigidity on drag force and mass transfer rates in model blades. *Limnol. Oceanogr.* **2014**, *59*, 2028–2041. [CrossRef]
48. Tsujimoto, T. Fluvial processes in streams with vegetation. *J. Hydraul. Res.* **1999**, *37*, 789–803. [CrossRef]
49. Tanaka, N. Vegetation bioshields for tsunami mitigation: Review of effectiveness, limitations, construction, and sustainable management. *Landsc. Ecol. Eng.* **2009**, *5*, 71–79. [CrossRef]
50. Shih, S.S.; Hong, S.S.; Chang, T.J. Flume Experiments for Optimizing the Hydraulic Performance of a Deep-Water Wetland Utilizing Emergent Vegetation and Obstructions. *Water* **2016**, *8*, 265. [CrossRef]
51. Westlake, D.F.; Dawson, F.H. The effects of autumnal weed cuts in a lowland stream on water levels and flooding in the following spring. *Verh. Int. Ver. Limnol.* **1988**, *23*, 1273–1277. [CrossRef]
52. Dawson, F.H. *Ecology and Management of Water Plants in Lowland Streams*; Report of the Freshwater Biological Association; Freshwater Biological Association: Ambleside, UK, 1989; Volume 57, pp. 43–60.
53. ASTM D790-03. In *Standard Test Methods for Flexural Properties of Unreinforced and Reinforced Plastics and Electrical Insulating Materials*; ASTM International: West Conshohocken, PA, USA, 2003.
54. Bialik, R.J.; Karpiński, M.; Rajwa, A.; Luks, B.; Rowiński, P.M. Bedform characteristics in natural and regulated channels: A comparative field study on the Wilga River, Poland. *Acta Geophys.* **2014**, *62*, 1413–1434. [CrossRef]
55. Fukushima, T.; Sato, K. Lodging of cabbage seedling due to its own weight. *Biosyst. Eng.* **2009**, *103*, 438–444. [CrossRef]
56. Falk, S.; Hertz, C.H.; Virgin, H.I. On the relation between turgor pressure and tissue rigidity. I. *Physiol. Plant.* **1958**, *11*, 802–817. [CrossRef]
57. Niklas, K.J. *Plant Biomechanics. An Engineering Approach to Plant Form and Function*; University of Chicago Press: Chicago, IL, USA, 1992; ISBN 0-226-58641-6.
58. Chambers, P.A.; Kalff, J. Light and nutrients in the control of aquatic plant community structure. I. In situ experiments. *J. Ecol.* **1987**, *75*, 611–619. [CrossRef]
59. Chambers, P.A. Light and nutrients in the control of aquatic plant community structure. II. In situ observations. *J. Ecol.* **1987**, *75*, 621–628. [CrossRef]
60. Zalewska-Gałosz, J. Occurrence and distribution of *Potamogeton* hybrids (Potamogetonaceae) in Poland. *Feddes Repert.* **2002**, *113*, 380–393. [CrossRef]
61. Nepf, H.M.; Koch, E.W.K. Vertical secondary flows in submersed plant-like arrays. *Limnol. Oceanogr.* **1999**, *44*, 1072–1080. [CrossRef]
62. Järvelä, J. Effect of submerged flexible vegetation on flow structure and resistance. *J. Hydrol.* **2005**, *307*, 233–241. [CrossRef]
63. Righetti, M. Flow analysis in a channel with flexible vegetation using double-averaging method. *Acta Geophys.* **2008**, *56*, 801–823. [CrossRef]
64. Kałuża, T.; Tymiński, T. Analysis of the flow resistance in zones with flexible vegetation. *Infrastruct. Ecol. Rural Areas* **2010**, *8*, 79–91. (In Polish)
65. Baptist, M.J. A flume experiment on sediment transport with flexible, submerged vegetation. In Proceedings of the International Workshop on RIParian FORest Vegetated Channels: Hydraulic, Morphological and Ecological Aspects, RIPFOR, Trento, Italy, 20–22 February 2003.
66. Velasco, D.; Bateman, A.; Redondo, J.M.; DeMedina, V. An open channel flow experimental and theoretical study of resistance and turbulent characterization over flexible vegetated linings. *Flow Turbul. Combust.* **2003**, *70*, 69–88. [CrossRef]

67. Poggi, D.; Katul, G.G.; Albertson, J.D. Momentum transfer and turbulent kinetic energy budgets within a dense model canopy. *Bound.-Layer Meteorol.* **2004**, *111*, 589–614. [CrossRef]
68. Huai, W.X.; Zeng, Y.H.; Xu, Z.G.; Yang, Z.H. Three-layer model for vertical velocity distribution in open channel flow with submerged rigid vegetation. *Adv. Water Resour.* **2009**, *32*, 487–492. [CrossRef]
69. Kubrak, E.; Kubrak, J.; Rowiński, P.M. Application of one-dimensional model to calculate water velocity distributions over elastic elements simulating Canadian waterweed plants (*Elodea Canadensis*). *Acta Geophys.* **2013**, *61*, 194–210. [CrossRef]
70. Kubrak, E.; Kubrak, J.; Kiczko, A. Experimental Investigation of Kinetic Energy and Momentum Coefficients in Regular Channels with Stiff and Flexible Elements Simulating Submerged Vegetation. *Acta Geophys.* **2015**, *63*, 1405–1422. [CrossRef]
71. Ortiz, A.C.; Ashton, A.; Nepf, H. Mean and turbulent velocity fields near rigid and flexible plants and the implications for deposition. *J. Geophys. Res.-Earth* **2013**, *118*, 2585–2599. [CrossRef]